Syntheses, crystal structures and magnetic properties of manganese(II)-hedp compounds involving alkylenediamine templates (hedp = 1-hydroxyethylidene-diphosphonate)

Hui-Hua Song,[a] Ping Yin,[a] Li-Min Zheng,*[a] James D. Korp,[b] Allan J. Jacobson,*[b] Song Gao[c] and Xin-Quan Xin[a]

[a] State Key Laboratory of Coordination Chemistry, Coordination Chemistry Institute, Nanjing University, Nanjing 210093, P. R. China. E-mail: lmzheng@netra.nju.edu.cn
[b] Department of Chemistry, University of Houston, Houston, TX 77204, USA. E-mail: ajjacob@uh.edu
[c] State Key Laboratory of Rare Earth Materials Chemistry and Applications, Peking University, Beijing 100871, P. R. China

Four new manganese(II) diphosphonates, $[NH_3(CH_2)_4NH_3][Mn(hedpH_2)_2]$ (**1**) and $[NH_3(CH_2)_nNH_3][Mn_2(hedpH)_2]\cdot 2H_2O$ [$n = 4$ (**2**), 5 (**3**), 6 (**4**)] (hedp = 1-hydroxyethylidenediphosphonate), have been synthesized under hydrothermal conditions and structurally determined by X-ray single crystal diffraction. Compound **1** consists of polymeric $Mn(hedpH_2)_2$ single chains built up from vertex-sharing MnO_6 octahedra and CPO_3 tetrahedra. The chains are cross-linked by very strong hydrogen bonds to form a three-dimensional network with large channels containing the diammoniumbutane cations. Compounds **2**–**4** can be considered as isomorphous from a chemical point of view, although **3** crystallizes in the non-centrosymmetric space group $P2_1$ while **2** and **4** are in the centrosymmetric space group $P2_1/n$. Each of the three compounds contains $Mn_2(hedpH)_2$ double chains. These double chains are held together by very strong hydrogen bonds, forming one-dimensional channels that host the diammonium alkane cations and lattice water. The effect of the alkane length of the templates on the channel size and the hydrogen bonding network is discussed. Magnetic measurements show that weak antiferromagnetic interactions are mediated between the manganese centers in all four compounds.

Recently, a rapid expansion in metal phosphonate chemistry occurred, in part due to their potential applications in ion exchange, catalysis and sensors.[1–4] Compared with their phosphate analogs, the tunable organic units in mono-phosphonate (RPO_3^{2-}), diphosphonate [$R(PO_3)_2^{4-}$] and other bifunctional phosphonates allow for the construction of a number of metal phosphonate materials with new architectures including open framework structures.[5–13] Among these, the manganese phosphonates are still rather limited in number, including $Mn(O_3PC_nH_{2n+1})\cdot H_2O$, $Mn(O_3PC_6H_5)\cdot H_2O$,[14] $Mn^{III}(HO_3P-C_6H_5)(O_3PC_6H_5)\cdot H_2O$,[15] $MnZn_2(O_3PCH_2CH_2CO_2)_2$,[16] Mn_3-$(O_3PCH_2CO_2)_2$ and $Mn_3(O_3PCH_2CH_2CO_2)_2$.[17,18]

As an extension of our systematic investigations of template influences on the structures of metal diphosphonates based on 1-hydroxyethylidenediphosphonic acid [hedpH$_4$, $H_2O_3PC(OH)$-$(CH_3)PO_3H_2$],[19] herein we report the syntheses and crystal structures of four new manganese(II) diphosphonates with formulas $[NH_3(CH_2)_4NH_3][Mn(hedpH_2)_2]$ (**1**) and $[NH_3(CH_2)_nNH_3][Mn_2(hedpH)_2]\cdot 2H_2O$ [$n = 4$ (**2**), 5 (**3**), 6 (**4**)]. The magnetic properties of all four compounds are also presented.

Experimental

Materials and methods

All the starting materials were reagent grade and used as purchased. The 50% aqueous solution of 1-hydroxyethylidene-diphosphonic acid (hedpH$_4$) was purchased from the Nanjing Shuguang Chemical Factory of China. The elemental analyses were performed on a PE 240C elemental analyzer. The infrared spectra were recorded on an IFS66V spectrometer with pressed KBr pellets. Thermal analyses were performed under nitrogen with a heating rate of 5 °C min^{-1} on a TGA–DTA V1.1B TA Inst 2100 instrument. Variable-temperature magnetic susceptibility data for **1**–**4** were obtained on polycrystalline samples (56.7 mg for **1**, 50.4 mg for **2**, 45.6 mg for **3** and 51.1 mg for **4**) from 2 to 300 K in a magnetic field of 5 kG using a MagLab System 2000 magnetometer. Diamagnetic corrections were estimated from Pascal's constants.[20]

Syntheses

Synthesis of $[NH_3(CH_2)_4NH_3][Mn(hedpH_2)_2]$ (1). A mixture of $MnCl_2\cdot 4H_2O$ (0.5 mmol, 0.0992 g), 50% hedpH$_4$ (1 cm^3), NaF (1 mmol, 0.0420 g) and H_2O (8 cm^3), adjusted to pH = 3.15 with 1,4-diaminobutane, was kept in a Teflon-lined autoclave at 110 °C for 2 d. After slow cooling to room temperature, colorless needle-like crystals were collected as a monophasic material, based on the powder X-ray diffraction pattern. Yield: 85% based on Mn. Found (calcd.) for $C_8H_{26}N_2MnO_{14}P_4$: C, 17.99 (17.36); H, 4.80 (4.70); N, 5.03 (5.06)%. IR (KBr, cm^{-1}): 3261–2966s(br), 1658m, 1619m, 1525m, 1500vw, 1469w, 1452w, 1402w, 1373m, 1286vw, 1268vw, 1115s, 1070s, 934m, 797m, 653w, 551m, 518m, 476w, 414w, 406w.

Synthesis of $[NH_3(CH_2)_4NH_3][Mn_2(hedpH)_2]\cdot 2H_2O$ (2). Hydrothermal treatment of a mixture of $MnCl_2\cdot 4H_2O$ (1 mmol, 0.1989 g), 50% hedpH$_4$ (1 cm^3), NaF (1 mmol, 0.0418 g) and H_2O (8 cm^3), adjusted to pH = 4.74 with 1,4-diaminobutane, in a Teflon-lined autoclave at 110 °C for 2 d resulted in pale pink crystals of compound **2** as a single phase. Yield: 85% based on Mn. Found (calcd.) for $C_8H_{28}N_2Mn_2O_{16}P_4$:

DOI: 10.1039/b200814a

C, 15.55 (14.96); H, 4.55 (4.57); N, 4.14 (4.27)%. IR (KBr, cm^{-1}): 3410s, 3374s, 3118–2780s(br), 1677m, 1638m, 1556s, 1484m, 1463vw, 1428w, 1392w, 1369w, 1297w, 1137s, 1080w, 1058w, 996s, 925s, 908s, 894s, 787s, 665m, 569s, 498w, 467w, 417s, 408s.

Synthesis of [NH$_3$(CH$_2$)$_5$NH$_3$][Mn$_2$(hedpH)$_2$]·2H$_2$O (3).

Hydrothermal treatment of a mixture of MnCl$_2$·4H$_2$O (1 mmol, 0.1977 g), 50% hedpH$_4$ (1 cm^3), NaF (1 mmol, 0.0425 g) and H$_2$O (8 cm^3), adjusted to pH ≈ 4 with 1, 5-diamino-pentane, in a Teflon-lined autoclave at 110 °C for 2 d resulted in pale pink crystals of compound 3 as a single phase. Yield: 87% based on Mn. Found (calcd.) for C$_9$H$_{30}$N$_2$Mn$_2$O$_{16}$P$_4$: C, 17.14 (16.47); H, 4.76 (4.57); N, 4.14 (4.27)%. IR (KBr, cm^{-1}): 3443s, 3330–2782s(br), 1674m, 1628m, 1562m, 1530m, 1472m, 1413w, 1372w, 1136s, 998s, 923s, 897s, 792s, 664w, 566s, 499w, 466w, 412s.

Synthesis of [NH$_3$(CH$_2$)$_6$NH$_3$][Mn$_2$(hedpH)$_2$]·2H$_2$O (4).

Hydrothermal treatment of a mixture of MnCl$_2$·4H$_2$O (1.5 mmol, 0.2967 g), 50% hedpH$_4$ (1 cm^3), NaF (1 mmol, 0.0420 g), 1,6-diaminohexane (4 mmol, 0.4624 g) and H$_2$O (8 cm^3) (pH = 4.72) in a Teflon-lined autoclave at 110 °C for 2 d resulted in pink crystals of compound 4 as a single phase. Yield: 82% based on Mn. Found (calcd.) for C$_{10}$H$_{32}$N$_2$Mn$_2$O$_{16}$P$_4$: C, 18.75 (17.92); H, 4.99 (4.78); N, 4.36 (4.18)%. IR (KBr, cm^{-1}): 3481s, 3119–2778s(br), 1668m, 1637m, 1561m, 1474m, 1393m, 1373w, 1127s, 1015s, 936s, 895s, 792m, 662m, 564s, 498w, 470w, 407s.

Crystallographic studies

Single crystals of dimensions 0.14 × 0.10 × 0.04 mm for 1, 0.25 × 0.06 × 0.04 mm for 2, 0.40 × 0.10 × 0.08 mm for 3 and 0.35 × 0.16 × 0.16 mm for 4 were used for structure determinations. The data were obtained by using a Siemens SMART platform diffractometer equipped with a 1K CCD area detector at 298 K (for 1) or 223 K (for 2–4). A hemisphere of data (1271 frames at 5 cm detector distance) was collected using a narrow-frame method with scan widths of 0.30° in ω and an exposure time of 30 s/frame for 1, 35 s/frame for 2 and 25 s/frame for 3 and 4. The first 50 frames were re-measured at the end of data collection to monitor instrument and crystal stability, and the maximum correction applied on the intensities was < 1%. The data were integrated using the Siemens SAINT program,[21] with the intensities corrected for Lorentz factor, polarization, air absorption, and absorption due to variation in the path length through the detector faceplate. Empirical absorption and extinction corrections were applied for all four compounds.

The structures were solved by direct methods and refined on F^2 by full-matrix least squares using SHELXTL.[22] All the non-hydrogen atoms were refined anisotropically except the C atoms of [NH$_3$(CH$_2$)$_6$NH$_3$]$^{2+}$ in 4, two of which were disordered. These disordered C atoms were refined isotropically. The H atoms were treated as riding atoms having isotropic displacement parameters related to the atom to which they are bonded. Crystallographic and refinement details are listed in Table 1, with selected bond lengths and angles in Table 2 for 1 and Table 3 for 2–4.

CCDC reference numbers 178161–178164.

See http://www.rsc.org/suppdata/dt/b2/b200814a/ for crystallographic data in CIF or other electronic format.

Results and discussion

Syntheses and preliminary characterizations

Under hydrothermal conditions, four new manganese diphosphonate compounds 1–4 have been prepared. The fluoride was added in order to improve the crystallization of the final prod-

ucts. The same compounds were obtained in the absence of NaF. When 1,4-diaminobutane was employed as a structure-directing agent, two phases could be obtained. At a molar ratio of Mn : hedp at 1.0–2.0 : 2.5, the pH plays a very important role in the formation of these two phases. When the pH is low (2–4), compound 1 appears as the dominant phase, however, increasing the pH to 4–6 in the same reaction mixture promotes the formation of compound 2. The preparations of 3 and 4 are much less sensitive to pH and the same products were obtained when the pH value of the reaction mixture ranged from 3 to 6 and the Mn : hedp molar ratio was 0.5–2.0 : 2.5.

The presence of the hedpH$_n$ ligand in compounds 1–4 is confirmed by a series of bands between 900 and 1200 cm^{-1} in their IR spectra, characteristic of the stretching vibrations of the phosphonate PO$_3$ groups, as well as the bands between 490–570 cm^{-1} arising from the phosphonate bending modes.[23,24] The broad bands around 3000 cm^{-1}, arising from the O–H stretching vibrations of H$_2$O, hydroxy group and the protonated phosphonate oxygens, suggest that extensive hydrogen bonds are present in all four compounds. Thermal analyses reveal that compounds 2–4 lose weight in a single step below 220 °C. The weight losses (5.56% for 2, 6.19% for 3, 5.31% for 4) are in agreement with the values calculated for the removal of two water molecules (5.61% for 2, 5.49% for 3, 5.38% for 4). No distinct weight loss was found for compound 1. Above 300 °C, the thermal decomposition behaviors of 1–4 are very similar, corresponding to the release of organic components and the collapse of the structure.

Crystal structure of 1

Compound 1 crystallizes in space group $P\bar{1}$. The structure consists of [NH$_3$(CH$_2$)$_4$NH$_3$]$^{2+}$ cations and chains of vertex-sharing MnO$_6$ octahedra and CPO$_3$ tetrahedra. A detail of the chain is illustrated in Fig. 1 with selected bond lengths and angles in
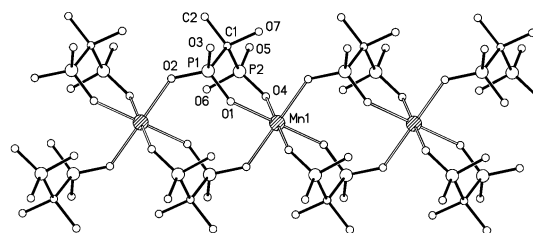

Fig. 1 A fragment of the Mn(hedpH$_2$)$_2$ chain in 1 with atom labeling scheme. All H atoms are omitted. The chain runs parallel to the a axis.

Table 2. The Mn atom occupies an inversion center, and has a slightly distorted octahedral environment. Each MnO$_6$ octahedron shares all of its vertices with six CPO$_3$ units from four equivalent hedpH$_2^{2-}$ groups. The Mn–O distances are between 2.110(2) and 2.224(2) Å, and the O–Mn–O angles are within 2° of their ideal values. The hedpH$_2^{2-}$ group, with singly protonated phosphonate groups at either end, links the Mn(II) ions in a chelating bridging mode using O(1), O(2) and O(4) atoms, forming infinite chains along [100] (Fig. 1). The hedpH$_2^{2-}$ ligand shows the usual pattern of P–O distances, with each phosphorus having two short bonds [av. 1.508(2) Å] and one long bond [av. 1.561(2) Å]. These values agree well with similar hedpH$_2$-metal complexes such as (enH$_2$)Zn(hedpH$_2$)$_2$·2H$_2$O,[25] (enH$_2$)Ni(hedpH$_2$)$_2$·2H$_2$O[26] and Pb(hedpH$_2$)·H$_2$O,[27] as well as the uncomplexed ligand in Na(hedpH$_3$)·H$_2$O[28] and hedpH$_4$·H$_2$O.[29] Some strain is evident in the O(1)–P(1)–O(2) and O(4)–P(2)–O(5) angles [av. 115.9(1)°], which are considerably larger than found in the free ligand[29] and may be a consequence of forming the chelating and bridging bonds comprising the polymeric chain. In the crystal lattice, these polymeric Mn(hedpH$_2$)$_2$ chains are cross-linked through very strong hydrogen bonds [av. O ⋯ O = 2.46 Å], forming large channels

Table 1 Crystallographic data

| Compound	1	2	3	4
Formula	$C_8H_{26}N_2MnO_{14}P_4$	$C_8H_{28}N_2Mn_2O_{16}P_4$	$C_9H_{30}N_2Mn_2O_{16}P_4$	$C_{10}H_{32}N_2Mn_2O_{16}P_4$
M	553.13	642.08	656.11	670.14
Crystal system	Triclinic	Monoclinic	Monoclinic	Monoclinic
Space group	$P\bar{1}$	$P2_1/n$	$P2_1$	$P2_1/n$
a/Å	5.3984(6)	5.6315(5)	5.6141(3)	5.6597(2)
b/Å	9.4004(10)	12.2419(10)	12.4252(6)	12.8273(6)
c/Å	10.4042(11)	16.4002(14)	16.4117(8)	16.4012(7)
a/°	65.237(2)			
β/°	80.868(2)	99.309(2)	98.925(1)	98.485(1)
γ/°	88.957(2)			
V/Å³	472.67(9)	1115.74(16)	1130.96(10)	1177.67(9)
Z	1	2	2	2
D_c/g cm⁻³	1.943	1.911	1.927	1.890
$F(000)$	285	656	672	688
μ(Mo-Kα)/cm⁻¹	11.13	14.97	14.79	14.22
Goodness of fit on F^2	1.026	1.034	1.066	1.068
R_1, $wR_2{}^a$ [$I > 2\sigma(I)$]	0.0310, 0.0825	0.0284, 0.0689	0.0246, 0.0612	0.0267, 0.0716
(all data)	0.0414, 0.0858	0.0395, 0.0731	0.0258, 0.0617	0.0280, 0.0723
$(\Delta\rho)_{max}$, $(\Delta\rho)_{min}$/e Å⁻³	0.375, −0.481	0.410, −0.354	0.367, −0.266	0.663, −0.557

^{a} $R_1 = \Sigma||F_o| - |F_c||/\Sigma|F_o|$. $wR_2 = [\Sigma w(F_o{}^2 - F_c{}^2)^2/\Sigma w(F_o{}^2)^2]^{1/2}$.

Table 2 Selected bond lengths [Å] and angles [°] for **1**

Mn(1)–O(4)	2.109(2)	Mn(1)–O(2B)	2.223(2)
Mn(1)–O(1)	2.225(2)	P(1)–O(2)	1.514(2)
P(1)–O(1)	1.516(2)	P(1)–O(3)	1.556(2)
P(1)–C(1)	1.850(3)	P(2)–O(4)	1.491(2)
P(2)–O(5)	1.510(2)	P(2)–O(6)	1.565(2)
P(2)–C(1)	1.844(3)		
O(4)–Mn(1)–O(2C)	89.71(8)	O(4)–Mn(1)–O(1)	89.08(8)
O(2B)–Mn(1)–O(1)	88.63(8)	O(2)–P(1)–O(1)	115.86(12)
O(4)–P(2)–O(5)	115.87(14)	P(1)–O(1)–Mn(1)	135.73(12)
P(1)–O(2)–Mn(1D)	138.14(13)	P(2)–O(4)–Mn(1)	134.94(13)

Symmetry transformations used to generate equivalent atoms: A, $-x$, $-y$, $-z$; B, $-x + 1$, $-y$, $-z$; C, $x - 1$, y, z; D, $x + 1$, y, z.
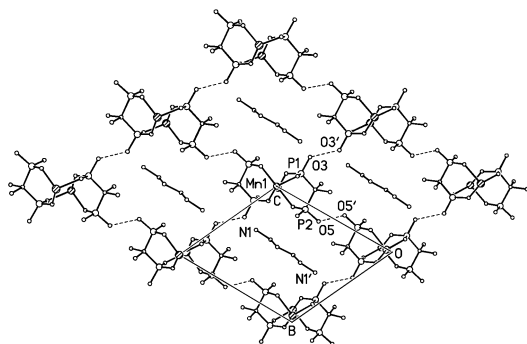
Fig. 2 View down the a axis showing the arrangement of the chains in **1**, and the 1,4-diammoniumbutane molecules which occupy the channels. Hydrogen bonds between chains are indicated by dashed lines.

along [100]. The diammonium cations occupy these channels, locked at each end by three NH $\cdots$ O hydrogen bonds (Fig. 2).

The arrangement of hydrogen atoms on the hedpH$_2{}^{2-}$ ligand in **1** is chemically simple, but crystallographically complicated. Atoms O(6) and O(7) have attached hydrogens 100% of the time, and are involved in intra-chain hydrogen bonding. Atoms O(3) and O(5), however, form the links which connect neighboring chains together, and are hydrogen bonded to their own symmetry relatives across inversion centers. These O(3)–H(3) $\cdots$ O(3′) and O(5)–H(5) $\cdots$ O(5′) moieties necessarily consist of one hydrogen for two oxygens, resulting in a 50% crystallographic occupancy for H(3) and H(5). The small amount of electron density involved could not be refined accurately, and so it is uncertain whether H(3) and H(5) actually reside on inversion centers [O $\cdots$ H $\cdots$ O] or are disordered around them [O–H $\cdots$ O vs. O $\cdots$ H–O]. Since H(3) and H(5)

Table 3 Selected bond distances [Å] and angles [°] for **2**, **3** and **4**

	2	3^a	4
Mn(1)–O(1)	2.116(2)	2.110(3)	2.117(2)
Mn(1)–O(2i)	2.120(2)	2.114(2)	2.123(2)
Mn(1)–O(4)	2.161(2)	2.160(2)	2.153(2)
Mn(1)–O(5)	2.176(2)	2.151(2)	2.130(2)
Mn(1)–O(7)	2.327(2)	2.354(2)	2.332(2)
Mn(1)–O(2t)	2.403(2)	2.418(2)	2.522(2)
P(1)–O(1)	1.517(2)	1.512(2)	1.515(2)
P(1)–O(2)	1.525(2)	1.526(2)	1.519(2)
P(1)–O(3)	1.549(2)	1.541(3)	1.547(2)
P(2)–O(4)	1.519(2)	1.511(2)	1.514(2)
P(2)–O(5)	1.518(2)	1.515(3)	1.526(2)
P(2)–O(6)	1.548(2)	1.547(3)	1.536(2)
P(1)–C(1)	1.844(3)	1.839(3)	1.835(2)
P(2)–C(1)	1.852(3)	1.849(3)	1.854(3)
Mn(1) $\cdots$ Mn(1i)	3.515	3.561	3.724
O(1)–Mn(1)–O(2i)	101.01(7)	99.10(9)	98.78(7)
O(1)–Mn(1)–O(2t)	93.44(7)	92.44(9)	92.29(6)
O(1)–Mn(1)–O(4)	90.88(7)	90.27(9)	89.01(7)
O(1)–Mn(1)–O(5)	167.37(7)	166.60(9)	164.89(7)
O(1)–Mn(1)–O(7)	89.86(7)	89.07(9)	87.29(7)
O(2i)–Mn(1)–O(2t)	78.17(7)	76.61(8)	73.73(7)
O(2i)–Mn(1)–O(4)	106.88(7)	109.85(10)	111.82(7)
O(2i)–Mn(1)–O(5)	88.42(7)	90.63(9)	92.12(7)
O(2i)–Mn(1)–O(7)	152.39(7)	150.93(8)	147.59(7)
O(2t)–Mn(1)–O(4)	172.61(7)	172.46(9)	174.04(7)
O(2t)–Mn(1)–O(5)	80.17(7)	80.93(9)	80.69(6)
O(2t)–Mn(1)–O(7)	75.88(6)	75.21(8)	74.24(6)
O(4)–Mn(1)–O(5)	94.42(7)	94.99(10)	96.67(7)
O(4)–Mn(1)–O(7)	98.16(7)	97.86(9)	100.02(7)
O(5)–Mn(1)–O(7)	78.06(7)	78.09(9)	77.96(6)
O(1)–P(1)–O(2)	116.18(11)	115.73(13)	115.71(10)
O(4)–P(2)–O(5)	116.59(11)	116.62(14)	115.62(10)
P(1)–O(1)–Mn(1)	133.25(11)	134.52(16)	135.03(11)
P(1)–O(2)–Mn(1i)	138.44(10)	137.37(13)	137.28(11)
P(1)–O(2)–Mn(1t)	115.13(10)	114.86(13)	112.67(9)
P(2)–O(4)–Mn(1)	135.03(11)	135.17(16)	137.35(11)
P(2)–O(5)–Mn(1)	118.12(10)	118.95(14)	120.49(10)
C(1)–O(7)–Mn(1)	106.43(14)	105.55(18)	106.70(13)
Mn(1)–O(2)–Mn(1i)	101.83(7)	103.38(10)	106.27(7)

^{a} Average of equivalent values in both independent Mn units. i: Atom generated by inversion center (for **2** and **4**). t: Atom generated by translation along the a axis (shown only when necessary to distinguish from type i atom).

appear in the difference Fourier map on the inversion centers, they were fixed at those locations arbitrarily. This type of extremely strong inter-chain hydrogen bonding will be discussed in greater detail for **2**–**4** (vide infra).

Crystal structures of 2–4

Compounds **2** and **4** are isostructural, both crystallizing in space group $P2_1/n$ with one-half formula unit per asymmetric unit. In **2** the diammonium molecule lies on an inversion center, while in **4** the diammonium is disordered over four separate orientations about the inversion center. Although compound **3** crystallizes in the non-centrosymmetric space group $P2_1$, examination of the unit cell constants indicates that the structures of all three complexes must be almost identical, which is found to be the case. Since the single 1,5-diammoniumpentane cation in the asymmetric unit of **3** crystallizes in an ordered conformation, the possibility of an inversion center is precluded and thus the crystallographic symmetry of the structure must be non-centrosymmetric. However, this is merely a crystallographic formality, and for most chemical purposes the three structures should be considered to be isomorphous. In fact, there is approximately a non-crystallographic pseudo-inversion center within the $Mn_2(hedpH)_2$ double chain in **3**. The two ends of the diammonium cation are in different orientations, however, which does cause some small variations in the bond distances and angles of the double chain. For purposes of comparison, the bonding geometries of the two independent halves of **3** will be averaged.

Compounds **2**, **3** and **4** each consist of a framework of $Mn_2(hedpH)_2$ and a diammonium alkane of different length (selected bond lengths and angles are collected in Table 3). While in **1** the hedp ligand is doubly protonated, in these three compounds the hedp is only singly protonated. This change in the overall charge of the anion is reflected in the Mn to hedp ratio (1 : 2 in **1** *vs.* 1 : 1 in **2**–**4**), which necessarily alters the arrangement of the components in the crystal lattice. Figs. 3 and 4 show fragments of the Mn(hedpH) chains in compounds
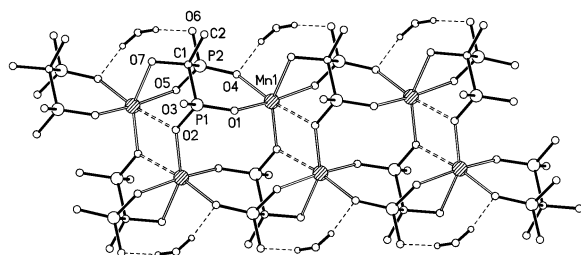

Fig. 3 A fragment of the $Mn_2(hedpH)_2$ double-chain in **2** with atom labeling scheme. All H atoms except those attached to water are omitted. Hydrogen bonds are indicated by thin dashed lines, and the long contacts between Mn and O(2) are indicated by double dashed lines. The chain runs parallel to the *a* axis.
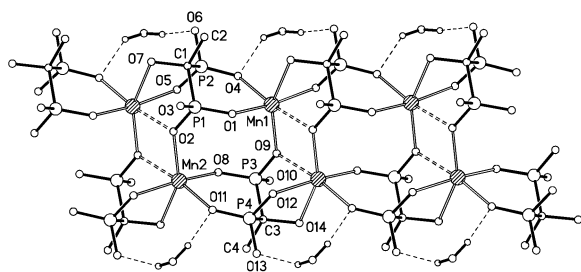

Fig. 4 A fragment of the $Mn_2(hedpH)_2$ double-chain in **3** with atom labeling scheme. Bonds are drawn as in Fig. 3.

2 and **3**, respectively. Compound **4** is labeled the same as **2**. In all three compounds, the Mn atom has a distorted octahedral geometry. As shown in Table 3, four of the Mn–O distances are normal length, one is intermediate, and one is extremely long. The intermediate length bond is to O(7), the ethylidene hydroxyl group, and would be expected to be weak due to its protonation and geometric constraints. The extremely long

Table 4 Distances between hydrogen bonded atoms [Å]

A(H) ⋯ B	2	3 [a]	4
O(3) ⋯ O(6) [b]	2.431(3)	2.435(3)	2.444(2)
N(1) ⋯ O(1)	2.812(3)	2.749(4)	2.71(2) [c]
N(1) ⋯ O(3)	2.849(3)	2.855(4)	2.91(3) [c]
N(1) ⋯ O(5)	2.767(3)	2.797(4)	2.76(3) [c]
O(7) ⋯ O(1w)	2.655(3)	2.704(4)	2.711(3)
O(1w) ⋯ O(4)	2.892(3)	2.942(3)	2.993(3)
O(1w) ⋯ O(6)	2.778(3)	2.812(4)	2.827(3)

[a] Average of equivalent values in both independent Mn units. [b] O(6)(H) ⋯ O(3) for **3** and **4**. [c] Average of both disordered NH_3 groups.

contact is to O(2), which is already bound to P(1) and another Mn atom. The reason why one Mn–O(2) distance is so much longer than the other is not entirely clear, but may involve some inflexibility on the part of the $hedpH^{3-}$ ligand. As can be seen in Fig. 3, each $hedpH^{3-}$ is at once tridentate, bidentate, and unidentate to three neighboring Mn ions, so some strain is to be expected.

The Mn(II) ions are bridged by $hedpH^{3-}$ groups to form a single chain, and two such chains are fused together by sharing edges of MnO_6 octahedra, thus forming a double chain. The closest Mn ⋯ Mn separation ranges from 3.515 Å in **2** to 3.724 Å in **4**. Very strong hydrogen bonds link these polymeric double chains together [O(3) ⋯ O(6) ≈ 2.44 Å, see Table 4]. Therefore the structure can be viewed as a three-dimensional open-network with channels along [100]. The diammonium cations and water molecules reside in the channels and are held in position by an intricate system of hydrogen bonds. A cross-section of the structure of **2** is shown in Fig. 5. The same phenomenon has been observed in both the Fe and Zn analogs.[25,30]

As can be seen in Table 3, the $hedpH^{3-}$ ligands in **2**, **3** and **4** are essentially the same, and show very little difference from the $hedpH_2^{2-}$ ligand in **1**. The same pattern of P–O bond distances is noted, as well as the large O(1)–P(1)–O(2) and O(4)–P(2)–O(5) angles. The close agreement between the bonding geometries of $hedpH_2^{2-}$ in **1** and $hedpH^{3-}$ in **2**–**4** is surprising, considering the radically different structures of the single chain and double chain. Even the P–O–Mn angles are quite similar, despite the striking differences in geometries of the fairly uniform Mn octahedron in **1** and the heavily distorted octahedra in **2**–**4**.

Hydrogen bonding in 2–4

These isomorphous complexes contain three general classes of hydrogen bonds: the OH ⋯ O links between double chains, the OH ⋯ O bonds involving the solvent waters, and the NH ⋯ O bonds which lock the diammonium molecules within the channels. As can be seen in Table 4, the three complexes have an identical pattern of hydrogen bonding, despite the varying lengths of the alkane backbone in the diammonium cations. The only systematic variations in the separation between the donor and acceptor atoms occur for N(1) ⋯ O(1), which shortens with increasing alkane length, and O(1w) ⋯ O(4), which lengthens. The O(1w) ⋯ O hydrogen bonds involving water range from 2.655 to 2.993 Å in the three complexes, which would be classified as moderately strong to moderately weak. The N ⋯ O separations ranging from 2.71 to 2.91 Å would be classified as strong to moderate.[31] All of these values fall well within the range of distances reported in the literature. The O(3) ⋯ O(6) separations, which range from 2.431 to 2.444 Å, are remarkably short however, and are among the strongest O ⋯ O type hydrogen bonds known. A similar bonding pattern was noted in **1**, as mentioned earlier. It is common for hydrogen phosphates and diphosphonates to

Table 5 Comparison of various parameters relating to channel size

	2	**3**	**4**
b axis/Å	12.242	12.425	12.827
O(3) $\cdots$ / $\cdots$ O(3)^a/Å	9.34	9.75	9.83
O(3) $\cdots$ O(6)/Å	2.431	2.435^b	2.444
P(1)–O(3) $\cdots$ O(6)/°	118.0	122.5^b	125.9
P(2)–O(6) $\cdots$ O(3)/°	133.0	134.3^b	140.1

^{a} Separation between opposing atoms across the channel containing the diammonium molecule. O(3) $\cdots$ / $\cdots$ O(10) for **3**. ^{b} Average of equivalent values in both independent Mn units.

Table 6 Diammonium torsion angles [°] and N $\cdots$ N separations [Å]

	1	**2**	**3**	**4**^{a}
N1–C–C–C	173	176	−170	−50
C–C–C–C	180	180	−169,−163	−163,−59,−169
C–C–C–N1i/N2	−173	−176	−56	−71
N $\cdots$ N	6.25	6.28	6.83	7.24
Max N $\cdots$ N^b	6.23	6.23	7.43	8.73

^{a} Average of both disordered orientations. ^{b} Ideal maximum separation, calculated assuming C–N = 1.47 Å, C–C = 1.54 Å, all angles = 109.5°, and all torsion angles = 180°.
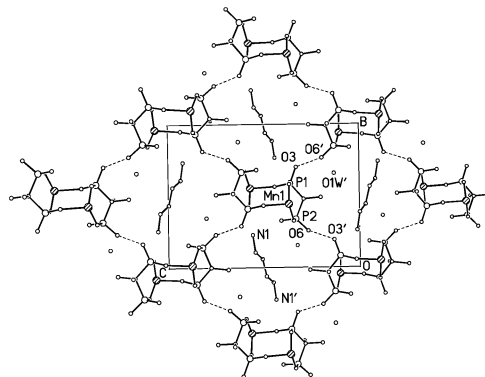
exhibit strong hydrogen bonds, and numerous examples have been reported.[31,32] In a survey of P–OH length *versus* O $\cdots$ O distance, Ferraris and Ivaldi concluded that for an O $\cdots$ O separation of 2.44 Å, the P–OH distance is about 1.54 Å, which is what we observe.[33] The most interesting feature of such strong hydrogen bonds is their ability to form "symmetric" bonds, in which the hydrogen atom is positioned exactly midway between the oxygens. Examples of this phenomenon would include potassium hydrogen maleate and lithium hydrogen phthalate, both with O–H distances of 1.20 Å. More frequently, however, the bond is "nearly symmetrical", examples of which would be $CaHPO_4$ [O–H/H $\cdots$ O = 1.18/1.28 Å] and $Na_3H(SO_4)_2$ [O–H/H $\cdots$ O = 1.16/1.28 Å].[31] For our complexes **2**, **3** and **4**, the hydrogen between O(3) and O(6) appeared in the difference density Fourier map at an O–H distance of about 1.10 Å. However, the hydrogen position could not be refined for **2** and **3** and had to be fixed at the map location. The hydrogen did refine nicely to O–H = 1.09 Å in **4**, which gives some reassurance that the fixed positions in **2** and **3** are accurate. Therefore, the O–H $\cdots$ O linkages between chains in **2**, **3** and **4** would appear to be strong, nearly symmetrical hydrogen bonds.

Comparison of 2–4

The purpose of synthesizing these three complexes was to determine the effects of small increases in the dication length on the overall crystal structure. Previously, we had determined that the analogous d^{10} Zn(II) complexes showed quite dramatic changes when different length templates were incorporated,[25] and it was decided to see if the d^5 Mn(II) complexes followed the same pattern. In Fig. 5 it is clear that the long axis of the diammonium cation is roughly parallel to the b axis of the unit cell, while the c axis is almost perpendicular. The a axis is parallel to the double chain axis, and is equal to the repeat length of the polymer unit. So, it would be expected that increasing the length of the cation would show the most effect on the b axial length, and this is found to be the case. Examination of the unit cell constants in Table 1 shows that the b axis lengthens with increasing cation length, while a and c are relatively unchanged. Since the bond distances in Table 3 show only small differences between the three complexes, it seems that the expansion along b must be due to changes in the hydrogen bonds linking the polymeric units together. The O(3) $\cdots$ O(6) separation is essentially constant, but the P–O $\cdots$ O angles change significantly, becoming closer to 180° as the dication chain increases in length. Another measure of channel expansion is the separation of opposing diphosphonate oxygen atoms such as O(3), and these values increase as expected from **2** to **4**. These parameters are summarized in Table 5. The ability of the channel in the open-network to expand is limited, and so the longer diammonium chains are forced to contort in order to fit into the same cavity. Figs. 6 and 7 show the environments about single dications in **3** and **4**, in the same orientation as Fig. 5, while Table 6 summarizes the torsional twists of the dication chains. Clearly, the diammoniumbutane molecules in **1** and **2** are maximally extended, with all torsion angles near 180°. Complex **3** has one end of the diammoniumpentane molecule sharply bent,

Fig. 5 View down the a axis showing the arrangement of the double-chains in **2**, and the 1,4-diammoniumbutane molecules and waters which occupy the channels. Hydrogen bonds between chains are indicated by dashed lines.
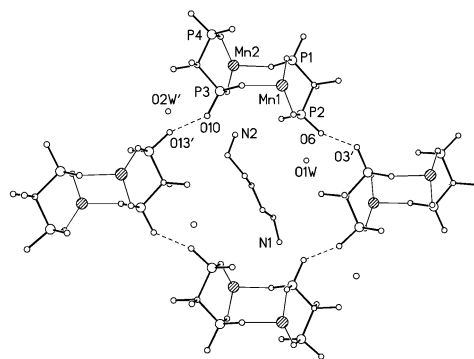

Fig. 6 View of a single channel in **3** showing the 1,5-diammoniumpentane and water molecules. The orientation is the same as in Fig. 5.
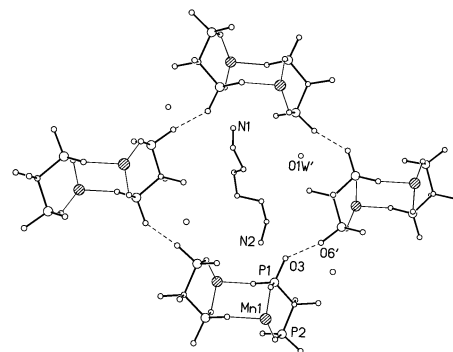

Fig. 7 View of a single channel in **4** showing the 1,6-diammoniumhexane and water molecules, oriented as in Fig. 5. Only one configuration of the disordered cation is shown.

while **4** has both ends bent. The amount of space saved by twisting can be estimated by comparing the N $\cdots$ N separation with the maximum which would be obtained if the molecule were maximally extended, as in **1** and **2**. These values are listed in Table 6, and show that the diammoniumpentane molecule

in **3** is shortened by 0.6 Å (8%) and the diammoniumhexane in **4** by 1.5 Å (17%). Each of the dications in **2**, **3** and **4** shows the same pattern of hydrogen bonding, despite having quite different torsional twists.

Comparison with Zn analogs

We have recently reported the crystal structure analyses of the Zn analogs of **2**, **3** and **4**, which will be referred to as **Z2**, **Z3**, and **Z4**.[25] These results show that **Z2** and **Z3** both crystallize in space group $P2_1/n$, with cell parameters approximately the same as **2**, **3**, and **4**. These five structures are isomorphous, taking into account the smaller bond radius of Zn vs. Mn. According to Shannon,[34] the effective ionic radius of Zn^{2+} is about 0.09 Å shorter than that of Mn^{2+} (high spin), and this is approximately what is found for five of the six metal–oxygen bonds. The sixth contact [listed in Table 3 as Mn(1)–O(2t)] is the only one which is longer for Zn than for Mn. In fact, for **Z3** the distance is so large (2.57 Å) that it was not even considered a weak bond anymore, making the Zn appear to be five-coordinate. At first this would seem to make the structures of **3** and **Z3** different, but careful analysis shows that the oxygen atoms in both structures are situated in very nearly the same positions. For example, in **3** the long Mn(1)–O(2t) contact and the bond trans to it [Mn(1)–O(4)] have an O · · · O separation of 4.55 Å, while the corresponding separation in **Z3** is 4.63 Å. Apparently, the uniform geometry of the diphosphonate ligand results in a nearly identical arrangement of oxygens about the Mn and Zn metal positions. The Zn atom is displaced within the O_6 sphere due to its smaller ionic radius, and thus appears farther from one oxygen.

The structure of **Z4** is completely anomalous, crystallizing in space group $P\bar{1}$. It consists of two separate types of double Zn(hedpH) chains, one containing distorted octahedral ZnO_6 coordination similar to **4**, and the other based on a distorted tetrahedral ZnO_4 coordination. These two types of chains are arranged in the lattice alternately, forming wider channels than in the other complexes. In fact, one of the two independent diammoniumhexane molecules has enough room to lie practically flat, with maximum N · · · N separation. This is possible because one set of inter-chain hydrogen bonds is not formed in **Z4**, resulting in only a two-dimensional network rather than the three-dimensional network formed in **4** and all the other complexes. It is not clear why the analogous Zn complexes **Z2** and **Z3** are isomorphous with the Mn complexes **2** and **3**, while **Z4** is so different from **4**, but perhaps the explanation lies in the stable electronic nature of the Zn ion. According to Cotton et al., Zn(II) "shows no stereochemical preferences arising from ligand field stabilization effects due to its d^{10} configuration. Therefore it displays a variety of coordination numbers and geometries based on electrostatic forces, covalence, and size".[35] Even the highly folded arrangement of the diammoniumhexane molecule exerts steric strain on the metal(hedp) network, as evidenced by the expansion of the b axis in **4**, and apparently this strain is enough to cause the formation of a different structural network in the case of highly adaptable Zn. While Mn(II) can also assume tetrahedral configurations, such as in $MnCl_4^{2-}$ and $MnBr_2(OPPh_3)_2$, they are generally not stable in contact with water and octahedral coordination is the preferred state.

The extreme variation between the crystal structures of **4** and **Z4**, and the quite different conformations of the diammonium molecules within them, lead to the question of how satisfactory long chain diammoniumalkanes are as templating agents. Recently Harrison et al., reported the structure of a complex of 1,3-diammoniumpropane with $Zn(HPO_4)_2$, wherein infinite zincophosphate chains are cross-linked by hydrogen bonded cations.[36] They found that the diammonium molecule bends at one end in order to optimize hydrogen bonding, much as in our structure **3**. However, they noted that a previously reported complex based on the same reactants contained a completely

different structure having a maximally extended diammonium cation as in our structure **2**,[37] and thus concluded that there was no significant control over the synthetic products in their reaction due to the flexible nature of the templating cation used. Our current results agree with this observation, and indicate that both electronic and crystal packing forces are able to overcome any specific structure-directing template effect of long chain diammoniumalkanes.

Chirality of 3

Reports of metal phosphonates having chiral structures are extremely rare. Two approaches can be used to introduce chirality into such structures, either by employing an organophosphonate made chiral by modification of the organic part or by using a suitable template. Using the first method, Bujoli and co-workers succeeded in synthesizing the first enantiomerically pure zinc phosphonate (R)-$Zn[O_3PCH_2P(O)(CH_3)$-$(C_6H_5)]$.[38] And by using a chiral organic amine as template, or a chiral metal complex, metal phosphates with necessarily chiral structures have been prepared.[39–41] A chiral tin phosphate $[CN_3H_6][Sn_4P_3O_{12}]$ in which an achiral template is involved has also been described.[42] However, as far as we are aware, no example has yet been reported of a chiral metal phosphonate directed by a template.

By employing diammoniumalkanes $NH_3(CH_2)_nNH_3$ ($n = 4, 5, 6$) as structure-directing agents, we have prepared the three isomorphous compounds **2**–**4**. The structures of **2** and **4**, with even numbers of methylene groups in the dication chain, crystallize in the centrosymmetric space group $P2_1/n$, while **3** having an odd number of methylene groups crystallizes in the chiral space group $P2_1$. Since a crystallographically ordered conformation of the dication having any even number of methylene carbons can conceivably lie about an inversion center while those having an odd number cannot, the trend is suggestive, however no general pattern should be inferred based on such a small number of experiments. Still, compound **3** appears to be the first example of a metal phosphonate with its chirality directed by an achiral organic template.

The $Mn_2(hedpH)_2$ chains in **2**–**4** are almost identical, each being composed of individual Mn(hedpH) units which are inherently chiral. While $hedp^{4-}$ is achiral, the extra hydrogen on $hedpH^{3-}$ creates a chiral center at C(1) since the two phosphate groups PO_3 and HPO_3 are inequivalent. In the solid state, even the presence of a symmetric O(3) · · · O(6) hydrogen bond between chains does not destroy this chiral center at C(1), since the three-center bonding geometry of O(2) on P(1) has no equivalent on P(2) [see Fig. 3]. The Mn atom is also a chiral center, technically, although this is not readily apparent until the disparity in the Mn–O bond lengths is taken into account. To help visualize this, the extremely long Mn–O bonds in Figs. 3 and 4 are shown as double-width dashed lines. In **2** and **4**, the two halves of the double chain (top horizontal strand vs. bottom strand in Fig. 3) are mirror images of each other, and the double chain is situated about inversion centers. This type of chain could be considered a racemic mix, with equal amounts of opposite chiralities present. In **3** however, the bonding geometries of Mn(1) and Mn(2) show a few significant differences, resulting in two crystallographically independent Mn(hedpH) units (see Fig. 4). For example, Mn(1)–O(2) = 2.387(2) Å and Mn(2)–O(9) = 2.449(2) Å, a difference of 31 standard deviations. And O(4)–Mn(1)–O(5) = 93.5(1)° while O(11)–Mn(2)–O(12) = 96.5(1)°, for a difference of 30σ.

A glance at Fig. 6 shows the most probable cause of these variations in bonding geometry — the asymmetric orientation of the diammonium molecules. As mentioned earlier, the 1,5-diammoniumpentane is slightly too long to fit into the natural channel formed between the double chains, and so it bends at the N(2) end. This bending actually creates a more favorable angle of approach for the hydrogen bonding between the three

ammonium hydrogens and the diphosphonate oxygens, as shown by the individual bonding parameters. For N(1), the three N–H ⋯ O angles are 120, 163 and 160°, while the corresponding angles for N(2) are 166, 153 and 152°. And the individual H ⋯ O distances for N(1) are 2.19, 1.96 and 1.99 Å vs. 1.86, 1.93 and 2.03 Å for N(2). Clearly the hydrogen bonds to N(2) are stronger and more uniform than those to N(1), which is supported by the fact that N(2) is positioned closer to the Mn atoms [av. 3.88 Å] than is N(1) [av. 3.98 Å]. The greatest difference in the corresponding hydrogen bonds is between N(1)–H(1A) ⋯ O(1) [2.19 Å, 120°] and N(2)–H(2E) ⋯ O(8) [1.86 Å, 166°]. The stronger pull on O(8) than O(1) apparently shifts the position of P(3) more than P(1) and results in a weaker Mn(2)–O(9) bond [2.449 Å] than Mn(1)–O(2) [2.387 Å]. Thus, the overall chiral arrangement of the metal phosphonate in **3** is a direct consequence of the asymmetric configuration of the otherwise achiral diammonium template.

Magnetic properties

The temperature dependent magnetic behaviors of **1–4** were investigated in the temperature range 300 to 2 K. Fig. 8 shows
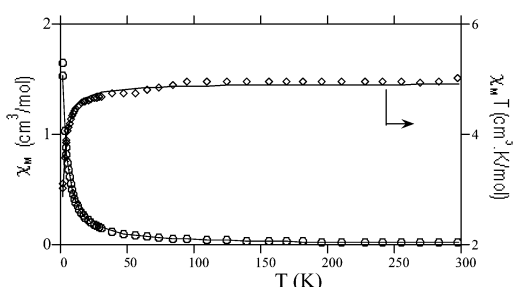
Fig. 8 The χ_M and $\chi_M T$ vs. T plot for **1**.

the χ_M and $\chi_M T$ vs. T plots for **1**. The effective magnetic moment (6.34 μ_B per Mn) at 298 K agrees with the theoretical value (5.91 μ_B) for an $S = 5/2$ ion. The Weiss constant, determined in the temperature range 80 to 300 K, is −0.97 K, suggesting a very weak antiferromagnetic exchange between the magnetic centers. This is confirmed by the slow decrease of $\chi_M T$ on cooling from room temperature. As the structure of **1** contains equally spaced linear chains of composition Mn(hedpH$_2$)$_2$ where the Mn(II) centers are bridged by O–P–O groups, the susceptibility data were analyzed by Fisher's expression for a uniform chain, with the classical spins scaled to a real quantum spin of $S = 5/2$.[20,43] A good fit was obtained, leading to parameters $g = 2.12$, $J = -0.18$ cm^{-1} (Fig. 8).

The magnetic behavior of **2** is shown in Fig. 9. Anti-

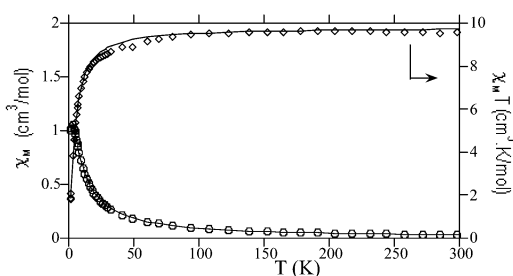**Fig. 9** The χ_M and $\chi_M T$ vs. T plot for **2**.

ferromagnetic exchanges are again observed, indicated by the continuous decrease of $\chi_M T$ on cooling. Considering that a double chain of composition Mn$_2$(hedpH)$_2$ is found in **2**, antiferromagnetic interactions between the Mn(II) centers can be propagated through both the μ-O bridges and the O–P–O groups within the double chain. Assuming that the exchange coupling through the O–P–O group is much weaker, the data

can be analyzed by an isotropic dimer model for two $S = 5/2$ ions based on the Heisenberg Hamiltonian $H = -J\mathbf{S_A}\cdot\mathbf{S_B}$.[20] A good fit was obtained with the parameters $g = 2.12$, $J = -0.67$ cm^{-1} (Fig. 9). The magnetic data for **3** and **4** were also analyzed by a similar dimer model to that for **2**. The parameters are $g = 2.08$, $J = -0.69$ cm^{-1} for **3** and $g = 1.98$, $J = -0.77$ cm^{-1} for **4**, respectively.

Conclusion

Four new manganese(II)-hedp complexes have been synthesized using three different diammoniumalkanes as templates. Each complex consists of a three-dimensional open-network of Mn(hedpH$_2$)$_2$ single chains (**1**) or Mn$_2$(hedpH)$_2$ double chains (**2–4**) linked together by very strong hydrogen bonds. The diammonium molecules reside within the large channels formed between chains, which expand slightly with increasing alkane length of the cation. This series of complexes is significantly different from the analogous Zn compounds, demonstrating that the structure-directing effect of long chain diaminoalkanes is limited by their inherent flexibility, which can be influenced in unpredictable ways by both electronic and crystal packing forces. Although the three double chain complexes are essentially isomorphous, the crystallization of compound **3** in a chiral space group proves that chiral metal phosphonates can be created by incorporating suitable achiral organic templates. Preliminary magnetic investigations show that only very weak antiferromagnetic interactions are mediated between the Mn centers in all four cases.

References

1 B. Zhang and A. Clearfield, *J. Am. Chem. Soc.*, 1997, **119**, 2751.
2 G. Alberti, *Comprehensive Supramolecular Chemistry*, ed., J.-M. Lehn, Pergamon, Elsevier Science, Ltd., Oxford, U.K., 1996, vol. 7.
3 J. L. Snover, H. Byrd, E. P. Suponeva, E. Vicenzi and M. E. Thompson, *Chem. Mater.*, 1996, **8**, 1490.
4 G. Cao, H. Hong and T. E. Mallouk, *Acc. Chem. Res.*, 1992, **25**, 420.
5 A. Clearfield, *Progress in Inorganic Chemistry*, ed., K. D. Karlin, John Wiley & Sons, Inc., New York, 1998, vol. 47, pp. 371–510.
6 V. Soghomonian, Q. Chen, R. C. Haushalter and J. Zubieta, *Angew. Chem., Int. Ed. Engl.*, 1995, **34**, 223.
7 D. L. Lohse and S. C. Sevov, *Angew. Chem., Int. Ed. Engl.*, 1997, **36**, 1619.
8 K. Maeda, J. Akimoto, Y. Kiyozumi and F. Mizukami, *Angew. Chem., Int. Ed. Engl.*, 1995, **34**, 1199.
9 J. Le Bideau, C. Payen, P. Palvadeau and B. Bujoli, *Inorg. Chem.*, 1994, **33**, 4885.
10 R. C. Finn and J. Zubieta, *J. Chem. Soc., Dalton Trans.*, 2000, 1821.
11 A. Distler, D. L. Lohse and S. C. Sevov, *J. Chem. Soc., Dalton Trans.*, 1999, 1805.
12 C. Serre and G. Ferey, *Inorg. Chem.*, 1999, **38**, 5370.
13 H. G. Harvey, S. J. Teat and M. P. Attfield, *J. Mater. Chem.*, 2000, **10**, 2632.
14 G. Cao, H. Lee, V. M. Lynch and T. E. Mallouk, *Inorg. Chem.*, 1988, **27**, 2781.
15 A. Cabeza, M. A. G. Aranda, S. Bruque, D. M. Poojary and A. Clearfield, *Mater. Res. Bull.*, 1998, **33**, 1265.
16 S. Drumel, P. Janvier, M. Bujoli-Doeuff and B. Bujoli, *New J. Chem.*, 1995, **19**, 239.
17 A. Cabeza, M. A. G. Aranda and S. Bruque, *J. Mater. Chem.*, 1998, **8**, 2479.
18 N. Stock, S. A. Frey, G. D. Stucky and A. K. Cheetham, *J. Chem. Soc., Dalton Trans.*, 2000, 4292.

19 L.-M. Zheng, H.-H. Song and X.-Q. Xin, *Comments Inorg. Chem.*, 2000, **22**, 129.
20 O. Kahn, *Molecular Magnetism*, VCH Publishers, Inc., New York, 1993.
21 SAINT Program for Data Extraction and Reduction, Siemens Analytical X-Ray Instruments Inc., Madison, WI 53719, 1994–1996.
22 G. M. Sheldrick, SHELXTL, Program for Refinement of Crystal Structures, Siemens Analytical X-Ray Instruments Inc., Madison, WI 53719, 1994.
23 K. L. Nash, R. D. Rogers, J. Ferraro and J. Zhang, *Inorg. Chim. Acta*, 1998, **269**, 211.
24 L. C. Thomas, *The Identification of Functional Groups in Organophosphorus Compounds*, Academic Press, London, 1994.
25 H.-H. Song, L.-M. Zheng, Z. Wang, C.-H. Yan and X.-Q. Xin, *Inorg. Chem.*, 2001, **40**, 5024.
26 H.-H. Song, L.-M. Zheng, C.-H. Lin, S.-L. Wang, X.-Q. Xin and S. Gao, *Chem. Mater.*, 1999, **11**, 2382.
27 J.-P. Silvestre, N. El Messbahi, R. Rochdaoui, N. Q. Dao, M.-R. Lee and A. Neuman, *Acta Crystallogr., Sect. C*, 1990, **46**, 986.
28 R. Rochdaoui, J.-P. Silvestre, N. Q. Dao, M.-R. Lee and A. Neuman, *Acta Crystallogr., Sect. C*, 1990, **46**, 2083.
29 V. A. Uchtman and R. A. Gloss, *J. Phys. Chem.*, 1972, **76**, 1298.
30 L.-M. Zheng, H.-H. Song, C.-H. Lin, S.-L. Wang, Z. Hu, Z. Yu and X.-Q. Xin, *Inorg. Chem.*, 1999, **38**, 4618.
31 G. A. Jeffrey, *An Introduction to Hydrogen Bonding*, Oxford University Press, Oxford, 1997.
32 C. V. K. Sharma and A. Clearfield, *J. Am. Chem. Soc.*, 2000, **122**, 4394.
33 G. Ferraris and G. Ivaldi, *Acta Crystallogr., Sect. B*, 1984, **40**, 1.
34 R. D. Shannon, *Acta Crystallogr., Sect. A*, 1976, **32**, 751.
35 F. A. Cotton, G. Wilkinson, C. A. Murillo and M. Bochmann, *Advanced Inorganic Chemistry*, 6th Edn., John Wiley and Sons, New York, 1999.
36 W. T. A. Harrison, Z. Bircsak, L. Hannooman and Z. Zhang, *J. Solid State Chem.*, 1998, **136**, 93.
37 S. Kamoun, A. Jouini, A. Daoud, A. Durif and J. C. Guitel, *Acta Crystallogr., Sect. C*, 1992, **48**, 133.
38 F. Fredoueil, M. Evain, M. Bujoli-Doeuff and B. Bujoli, *Eur. J. Inorg. Chem.*, 1999, 1077.
39 K.-H. Lii, Y.-F. Huang, V. Zima, C.-Y. Huang, H.-M. Lin, Y.-C. Jiang, F.-L. Liao and S.-L. Wang, *Chem. Mater.*, 1998, **10**, 2599.
40 D. A. Bruce, A. P. Wilkinson, M. G. White and J. A. Bortrand, *J. Chem. Soc., Chem. Commun.*, 1995, 2059.
41 M. J. Gray, J. D. Jasper, A. P. Wilkinson and J. C. Hanson, *Chem. Mater.*, 1997, **9**, 976.
42 A. Ayyappan, X. Bu, A. K. Cheetham and C. N. R. Rao, *Chem. Mater.*, 1998, **10**, 3308.
43 M. E. Fisher, *Am. J. Phys.*, 1964, **32**, 343.